Applied Surface Science Advances 25 (2025) 100694

Contents lists available at ScienceDirect

Applied Surface Science Advances

journal homepage: www.sciencedirect.com/journal/applied-surface-science-advances

Full Length Article

# Epitaxial growth of non-polar a-plane ZnO and aluminium-doped ZnO on r-sapphire using the intermittent spray pyrolysis methodology

Cerine Treesa Russel *, Carmen Martinez Tomas, Vicente Muñoz Sanjosé

*Department de Fisica Aplicada i Electromagnetisme, Universitat de Valencia, C/ Dr. Moliner 50, Burjassot 46100, Valencia, Spain*

ARTICLE INFO

*Keywords:*
Epitaxial thin film
Non-polar Zinc oxide
Aluminum doped a-Zinc oxide
Spray pyrolysis
Morphological and structural properties
Electrical-Hall measurements

ABSTRACT

In this article, we highlight the epitaxial growth of non-polar a-plane ZnO and aluminium-doped ZnO using the low-cost, non-vacuum and highly up-scalable intermittent spray pyrolysis technique. We successfully deposited epitaxial ZnO and Al: ZnO thin films over r-sapphire using our optimized homemade Spray Pyrolysis setup. The epitaxial relationships are those usually found in the samples grown by the conventional well established epitaxial growth methods, that is, with a $ZnO(11\bar{2}0)\|\ Al_2O_3(01\bar{1}2)$ out-of-plane direction. We investigated the effect of growth temperature on the growth of ZnO over r-sapphire substrate in the temperature range 300 °C to 600 °C and found that under the growth conditions that were used, there was an optimum growth temperature range of 450 °C-500 °C in which we could grow very compact uniform epitaxial ZnO thin films. At both, lower and higher growth temperatures, due to the instability induced in growth conditions (Ehrlich-Schwoebel effect and stress-induced instability, respectively), there was surface roughening. The effect of aluminium doping on ZnO was also investigated for the optimum growth temperatures 450 °C and 500 °C using morphological, structural and electrical (Hall measurements) characterisation. The Al:ZnO sample with a nominal aluminium concentration of 1 % without any post-deposition treatments had a carrier concentration of $5.03 \times 10^{19}$ $cm^{-3}$ and mobility of 10 $cm^2/V{\cdot}s$.

## 1. Introduction

ZnO is a group II-VI semiconductor material with a direct bandgap of 3.37 eV at room temperature with a large excitonic binding energy of 60 meV. ZnO has a wurtzite structure, the same crystallographic structure as GaN. This characteristic joined to a lattice mismatch as low as <1.8 %, makes ZnO a potential substrate for the growth of GaN and, also and more significantly, a promising material in electronic devices [1].

ZnO films grown in the (0001) direction, that is, along the c-axis, suffer from the inherent problem of spontaneous polarisation and strain-induced piezoelectric polarisation. The polar nature of c-plane ZnO leads to the generation of large electrostatic fields (giving rise to large sheet charges at the interfaces), which reduces the overlap between the electron and hole wave functions in the quantum well structures. This behaviour leads to reduced electron-hole recombination probability, being a source for the deterioration of the device performance. The problem of spontaneous polarisation can be eliminated by using the non polar planes of ZnO [2]. It is worth noting that the in-plane biaxial strain of polar c-ZnO film is isotropic, whereas the in-plane biaxial strain of non-polar a-ZnO is anisotropic due to the asymmetry associated with the wurtzite crystal structure [3]. This anisotropic strain in the non-polar ZnO can be of interest in LEDs [4] and polarisation-sensitive photodiodes [5]. In general, ZnO is an n-type semiconductor due to the presence of intrinsic defects like zinc interstitials and oxygen vacancies. The n-type conductivity of zinc can be enhanced by doping with group III elements like boron, aluminium, gallium etc. Among these elements, aluminium-doped ZnO (AZO) enhances the suitability of ZnO for opto-electronics, providing a non-toxic, affordable transparent conducting oxide with higher charge carrier concentration. This is because $Al^{3+}$ ions act as donors, introducing additional free electrons in the crystal structure thereby resulting in improved electrical conductivity, while still maintaining the properties of high transparency in the visible region due to the close covalent bond length of Al-O (0.192 nm) to that of Zn-O (0.197 nm) [6].

Epitaxial ZnO compounds are useful for the fabrication of devices like light-emitting diodes, laser diodes, piezoelectric devices etc. Usually, techniques like molecular beam epitaxy [7], atomic layer deposition [8], sputtering [9], pulsed laser deposition [3,10], metal-organic

* Corresponding author.
*E-mail address:* Cerine.Russel@uv.es (C.T. Russel).

https://doi.org/10.1016/j.apsadv.2025.100694
Received 3 December 2024; Received in revised form 29 December 2024; Accepted 7 January 2025
Available online 17 January 2025

chemical vapour deposition [11–13] are used to grow high-quality epitaxial ZnO films. But these techniques, despite their ability to grow high-quality films, tend to be expensive due to their high operational costs. Spray pyrolysis is another thin film deposition technique, in which the precursor solution is atomized and then sprayed onto the substrate, which is maintained at the growth temperature. So, the precursors undergo pyrolysis, that is, they decompose through specific reactions, and form the required material at the substrate. This is a very simple, up-scalable technique with lower operational costs. Achieving dense, uniform films that are free of pinholes is one of the main challenges of spray pyrolysis. This difficulty justifies its limited popularity in the epitaxial thin film growth. Nevertheless, spray pyrolysis has previously been used to grow epitaxial films of some materials. J.J.Chu et al. reported the epitaxial growth of high $T_c$ superconducting Y-Ba-Cu-O thin films on (001) MgO by chemical spray pyrolysis [14]. Homoepitaxial films of gallium arsenide were grown on (001) GaAs from a single source organometallic precursor using a modified spray pyrolysis process by A. A.Wernberg et al. They used a hybrid of spray pyrolysis and conventional organometallic chemical vapour deposition, introducing the precursor into the hot wall reactor as a mist [15]. S.T. Zhang et al. grew epitaxial fluorine doped tin oxide (FTO) using ultrasonic spray pyrolysis on (110) rutile $TiO_2$ single crystals [16]. A. Ainabayev et al. fabricated high-quality epitaxial $VO_2$ thin films on c-plane sapphire [17]. However, the possibilities of conventional spray pyrolysis setups for epitaxial growth of thin films remain an open subject, thus presenting both an opportunity to reduce production costs in device fabrication and an intriguing academic challenge.

In this paper, after meticulously controlling the growth parameters, we report the growth of epitaxial non-polar a-plane ZnO and aluminium-doped ZnO over r-sapphire using the spray pyrolysis methodology by means of an intermittent process. We carried out a systematic investigation to understand the effect of temperature on the growth of ZnO over r-sapphire substrates. It was found that the growth in the temperature range 450 °C and 500 °C yielded ZnO films which had uniform homogeneous smooth thin film-like morphology. The excellent structural properties of these films are confirmed by the high-resolution X-ray diffraction (HR-XRD) measurements. Based on this information, the study was extended to the growth of aluminium-doped ZnO (AZO), at both those temperatures, to understand the effect of aluminium doping, while still maintaining excellent morphological and structural properties. The morphological, structural and electrical characterization of these AZO samples was carried out. Based on the results of electrical characterisation, it was found that the charge carrier concentration of the AZO samples grown at 450 °C was greater than that of those grown at 500 °C . To explain this behaviour, we suggest a mechanism to explain the improved electrical properties at lower growth temperatures based on the thermal decomposition and desorption of the aluminium precursor and its availability near the surface for lattice incorporation.

## 2. Experimental

The epitaxial ZnO thin film deposition was done using a relatively simple homemade spray pyrolytic setup. The rate at which the precursor solution was fed into the spray gun (Nordson) was modulated by a Syringe pump (New Era Pump Systems, NE300) and Nitrogen (99.99 %) was used as the carrier gas to disperse the solution onto the r-sapphire substrate (CrysTec) kept on the substrate heater whose temperature was controlled by two Eurotherm PID temperature controllers. The Nitrogen gas pressure was set to 1.6 bar with the carrier gas flow set to 4 lpm by a flowmeter (Brooks Instrument) and the nozzle to substrate distance set to 17 cm. To understand the effect of temperature on the ZnO growth, 0.2 M precursor solution, prepared by dissolving Zinc acetate dihydrate (Analytical Reagent grade, Fisher Scientific) in methanol (Analytical Reagent, VWR BDH Chemicals) was sprayed onto the r-sapphire substrates at different temperatures between 300 °C to 600 °C with a step size of 50 °C . 6 ml of the precursor solution was sprayed with a flow rate of 1 ml/min by intermittent spraying, where each 1 min spraying was followed by a 1 min interval. Then, once the required solution was deposited, the sample was allowed to remain at the growth temperature for 10 min, after which they were allowed to gradually cool down. A similar growth protocol of intermittent spraying was used for the growth of Aluminium doped ZnO (AZO) as well. The precursor solutions were prepared from the stock solutions of Zinc acetate dihydrate (Analytical Reagent grade, Fisher Scientific) and aluminium acetylacetonate (97 %, Acros organics) prepared using the solvent which is a mixture of methanol (Analytical Reagent, VWR BDH Chemicals) and glacial acetic acid (Analytical reagent grade, Fischer Scientific) in 97:3 ratio, with different concentrations of Aluminium (between 0 mol% and 3.5 mol%).

Taking in mind the results relative to the morphology of undoped ZnO, which we will analyse in the following section, for the growth of aluminium doped ZnO (AZO), 12 ml precursor solution was deposited by a flow rate of 1 ml/min on r-sapphire substrate at 450 °C and 500 °C.

The film morphology and cross-sectional thickness of the samples were determined by scanning electron microscopy using a Hitachi S4800. The 2θ-ω scans and pole figure measurements were done using a Panalytical X-Pert MRD diffractometer with Cu Kα radiation ($\lambda$ = 1.54056 Å). Parallel and monochromatic irradiation of the sample was ensured by a parabolic mirror and a 4-bounce hybrid monochromator situated at the incident beam. The carrier concentration, resistivity and mobility were measured in van der Pauw geometry with a DC magnetic field intensity of 1 Tesla using a LakeShore Cryotronics FastHall measurement system.

## 3. Results and discussion

### 3.1. Morphological studies

The morphology and the cross-sectional views of the undoped ZnO grown at different temperatures are shown in Fig. 1. At 300 °C, the surface has a lot of flake-like structures on the surface, but as the growth temperature is increased, the size of the grains increase and plate-like formations appear at 400 °C. If the temperature is increased further, at 450 °C and 500 °C, the thin films acquire a very compact and flat uniform surface. At higher temperatures, 550 °C and 600 °C, additional structures grow above the thin film layer, which therefore has reduced smoothness than before.

In the deposition method proposed here, a forced diffusion of the precursor vapour by the nitrogen carrier gas takes place. Depending on the temperature of the substrate placed on the hot plate, the complete pyrolysis of the precursors occurs at different regions. Ideally, we want the precursors to dissociate just above the surface of the substrate in order to obtain good-quality thin films. Higher growth temperatures favour more homogeneous nucleation, whereas lower growth temperatures result in inhomogeneous nucleation, but favour the growth process, forming larger grains. So initially, as the temperature increases, the nucleation is not very homogeneous on the substrate, resulting in flake-like formations. But as the temperature increases, we can see the increase in the size of the grains, forming larger plate-like structures. When the temperature is increased even further (between 450 °C and 500 °C), the results indicate that proper pyrolysis has occurred, with homogenous nucleation and low dispersion of the morphology, resulting in compact film-like morphology. At even higher temperatures, the stress-induced instability dominates the surface growth, which results in the formation of additional structures on the surface, thereby increasing surface roughness. So, as the morphology evolves with the growth temperature, the film surface will be rougher at both lower and higher temperatures. Z. J. Liu and Y. G. Shen studied the effect of temperature on the surface roughening of thin films and explained that, for thin film growth at lower temperatures, the surface would be rough due to the Ehrlich-Schowbel (E-S) effect, while at higher temperatures, the roughening is caused by stress-induced instability [18]. The surface roughness is caused due to unstable growth conditions. At lower growth

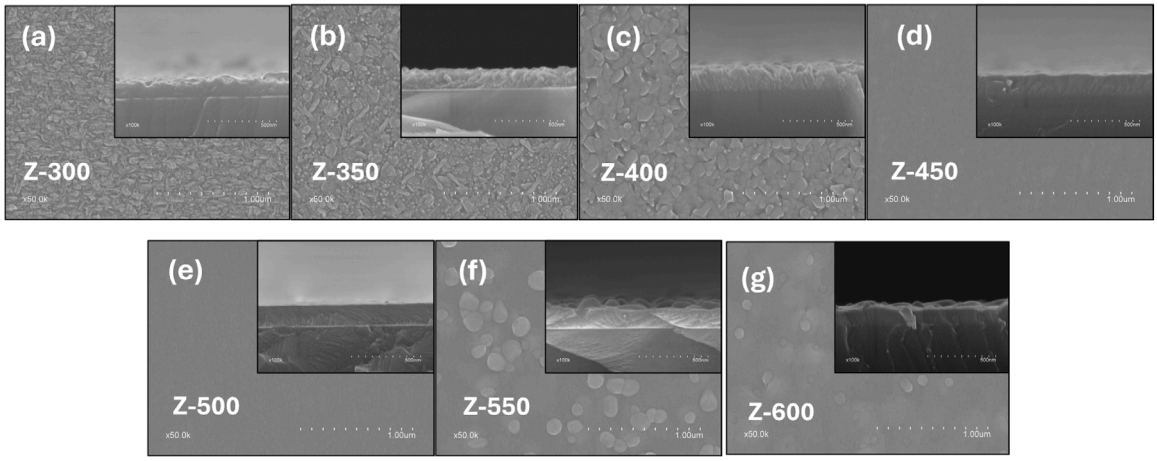


**Fig. 1.** Growth of undoped ZnO at different temperatures(a) 300 °C (b) 350 °C (c) 350 °C (d) 450 °C (e) 500 °C (f) 550 °C (g) 600 °C.

temperatures, the Ehrlich-Schwoebel (E-S) barrier plays a role in creating this instability. E-S barrier is a potential barrier that tries to block an adatom from diffusing over a step edge from the upper to the lower terrace, thereby, inducing an uphill particle current [19]. At high deposition temperatures, this instability in growth conditions is caused if there exists a stress due to lattice mismatch between the film and the substrate [18]. So, with the experimental conditions that we used, in the temperature region between 450 °C and 500 °C, we were able to grow very compact uniform ZnO thin films. Similar conditions were maintained for the growth of Al-doped ZnO in order to have the best conditions for obtaining a good morphology.

The morphology of the samples of aluminium-doped ZnO grown at both 450 °C and 500 °C is shown in Fig. 2 and Fig. 3. It could be seen that the morphology evolved from thin film-like morphology, to granular-like structures, with more grain boundaries as the aluminium content increased.

### 3.2. XRD analysis

In XRD patterns, all the observed diffraction peaks could be indexed to ZnO wurtzite structure, and no other impurity phase was found. The 2θ-ω scans showed that all the ZnO samples grown on r-sapphire at different temperatures, from 300 °C to 600 °C exhibit an out-of-plane preferential growth orientation in the $[11\bar{2}0]$ direction, according to previous studies [21].

In order to assess that there is also an in-plane orientation of the ZnO cell with respect to the r-sapphire substrate, pole figure measurements were made at 2θ=31.770° and 2θ=41.685° to obtain the $ZnO(10\bar{1}0)$ and the $Al_2O_3(0006)$ reflections (see Fig. 4(a)). All samples exhibited only two poles at Ψ=30°, separated by ± $90^0$, which confirms a clear in-plane orientation. The epitaxial resulting relationships of the samples were

$$ZnO(11\bar{2}0)\| Al_2O_3(01\bar{1}2)(\text{out}-\text{of}-\text{plane direction})$$

$$ZnO[0001]\| Al_2O_3[01\bar{1}\bar{1}]\ (\text{c}-\text{axis of ZnO direction})$$

$$ZnO[\bar{1}100]\| Al_2O_3[2\bar{1}\bar{1}0]\ (\text{m}-\text{axis of ZnO direction})$$

which indicates that the relative position of the ZnO cell and the surface of the r-sapphire is that shown in Fig. 4(b). Pole figure measurements made on AZO films (not shown) revealed that these samples showed the same epitaxial relations as the undoped ZnO thin films.

The measured inclination angle between the $Al_2O_3(01\bar{1}2)$ and $Al_2O_3(0006)$ planes is 57.61°. However, a small shift of 0.78° is observed between the $ZnO(11\bar{2}0)$ and the $Al_2O_3(01\bar{1}2)$ planes, giving rise to an angle between the $ZnO[11\bar{2}0]$ and the $Al_2O_3$ [0006] directions of 58.39°.

The optimum growth temperature range for ZnO films can be deduced form Fig. 5(a), (b) and (c). It can be seen in Fig. 5(a) that for temperatures lower than 400°, some additional ZnO peaks with low intensity, corresponding to the $ZnO(0002)$ and the $ZnO(10\bar{1}2)$ planes, were detected. In Fig. 5(b) it could be observed that the intensity of the $ZnO(11\bar{2}0)$ peak increased with the growth temperature reaching a maximum at 400 °C to 550 °C, which indicates that this range provides more favourable conditions for the growth of epitaxial ZnO films over r-

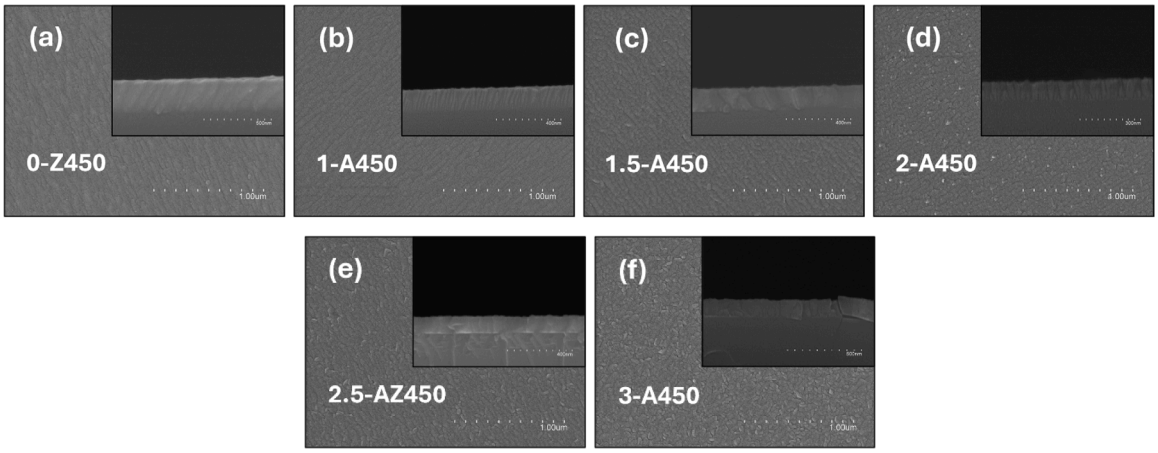


**Fig. 2.** Growth of AZO grown at 450 °C with different nominal concentrations of Aluminium (a) 0 % (b) 1 % (c) 1.5 % (d) 2 % (e) 2.5 % (f) 3 %.

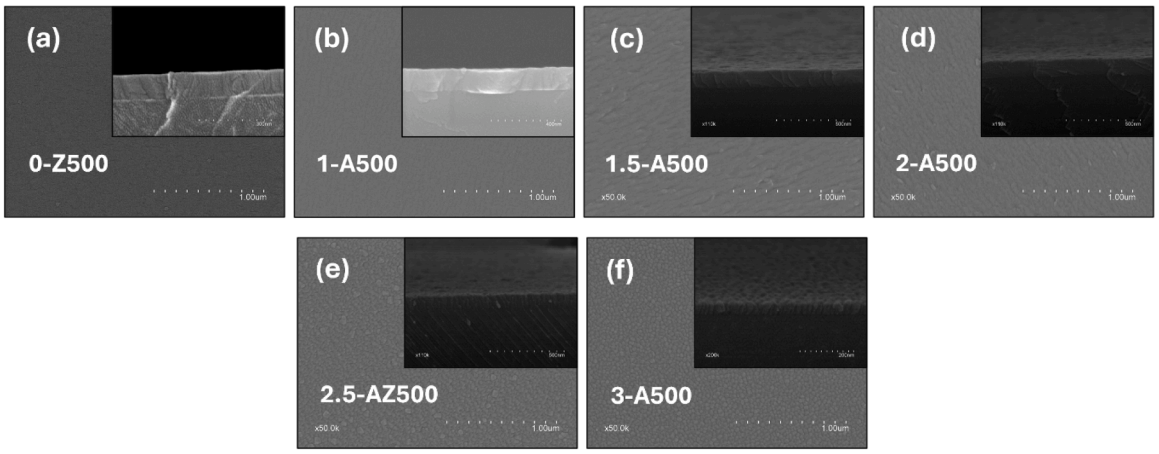


**Fig. 3.** Growth of AZO grown at 500 °C with different nominal concentrations of Aluminium (a) 0 % (b) 1 % (c) 1.5 % (d) 2 % (e) 2.5 % (f) 3 %.

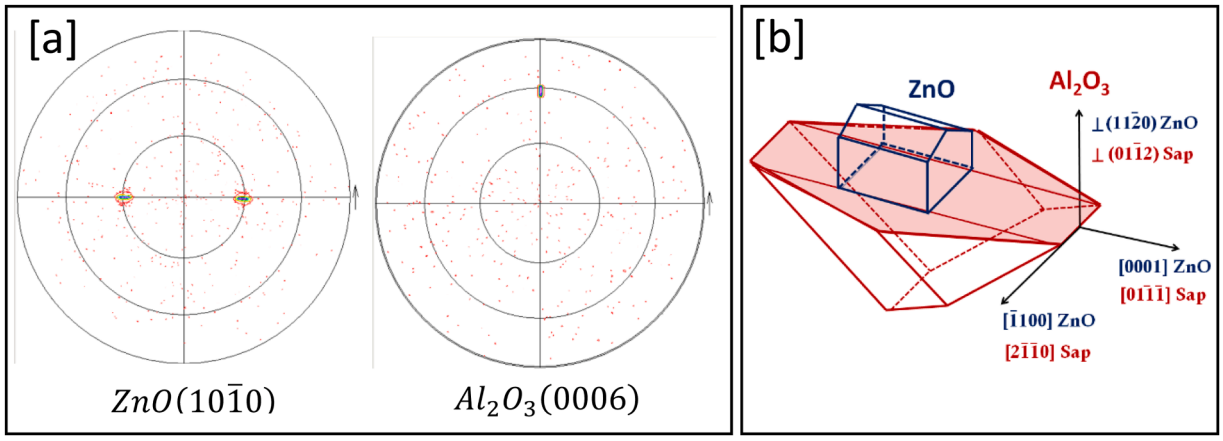


**Fig. 4.** (a) Pole figures of the ZnO$(10\bar{1}0)$ the $Al_2O_3(0006)$ reflections on films grown at 450 °C. (b) Schematic representation of the ZnO cell on the surface of r-sapphire [20].

sapphire substrates. It has to be noted that very narrow substrate peaks (visible when in linear scale) and the shift in the relative inclination between the $ZnO(11\bar{2}0)$ and the $Al_2O_3(01\bar{1}2)$ planes make it difficult for both peaks to be seen at the same time, that is why, it is seen only in certain cases like here in the case of sample grown at 600°C.

For each main peak of ZnO, after the optimization on the ω, 2θ and inclination angle, the full width at the half maximum (FWHM) was determined. In Fig. 5(c) it can be seen that this value decreases with increasing growth temperature, thus indicating an improvement of the crystallinity of samples. The sudden drop in the FWHM values for growth temperatures greater than 350 °C, indicates that for the deposition methodology used, growth temperatures higher than 350 °C are required to obtain good-quality ZnO thin films. B.P. Zhang et al. also discussed a similar observation in their study [21]. The obtained lowest FWHM values, namely $0.83^0$, $0.67^0$, and $0.78^0$, corresponds to 500 °C, 550 °C and 600 °C, respectively, that is, samples with higher growth temperatures. The FWHM values obtained in this paper are comparable to those obtained by means of some of the well-established epitaxial thin film deposition techniques, like MOCVD [11] and pulsed laser deposition [7]. The incorporation of aluminium content leads to an increase of the FWHM values with increasing nominal aluminium concentration as shown in Fig. 5(d). This increase in the FWHM values is because of the decreasing crystallinity of the AZO samples with increasing nominal aluminium content.

As said, a-ZnO films grown on r-sapphire substrates exhibit anisotropic in-plane strain. This distortion originates from the anisotropic in-plane lattice mismatch and from the different expansion thermal coefficients between layer and substrate. This combined anisotropy leads to an orthorhombic distortion of the unit cell, resulting in a compressive strain in the out-plane direction [21]. This out-plane strain can be evaluated as $\varepsilon_{110} = (a\text{-}a_0)/\ a_0 \times 100$ %, where $a_0$ =3.24982(9) Å is the bulk ZnO lattice parameter (JCPDS card 36–1451) [22] and "a" is the calculated a-lattice parameter in the out-plane direction. The variation of the strain in this direction is represented in Fig. 5(e). Until 450 °C, the compressive stress seems to be accumulating (reaching a minimum value of a-lattice parameter=3.243 ±0.001 Å), but in the temperature range of 450 °C and 600 °C, there appears to be a reduction in the compressive stress with increasing deposition temperature. Because of the higher thermal expansion coefficient of ZnO than that of sapphire [11] and the orthorhombic distortion of the ZnO cell, it results in a complex lattice mismatch between ZnO and sapphire, as a function of temperature, thereby resulting in smaller residual strain at higher growth temperatures.

### 3.3. *Electrical characterisation*

Table 1 shows the Hall effect measurement (using van der Pauw geometry) made on aluminium-doped ZnO films grown on r-sapphire substrate at 450 °C (Fig. 6(a)), and 500 °C (Fig. 6(b)). Aluminium can act as a donor dopant, as $Al^{3+}$ can substitute $Zn^{2+}$ in the lattice (substitutional doping), or rather can take one of the interstitial positions (interstitial doping), generating one free carrier for each dopant atom

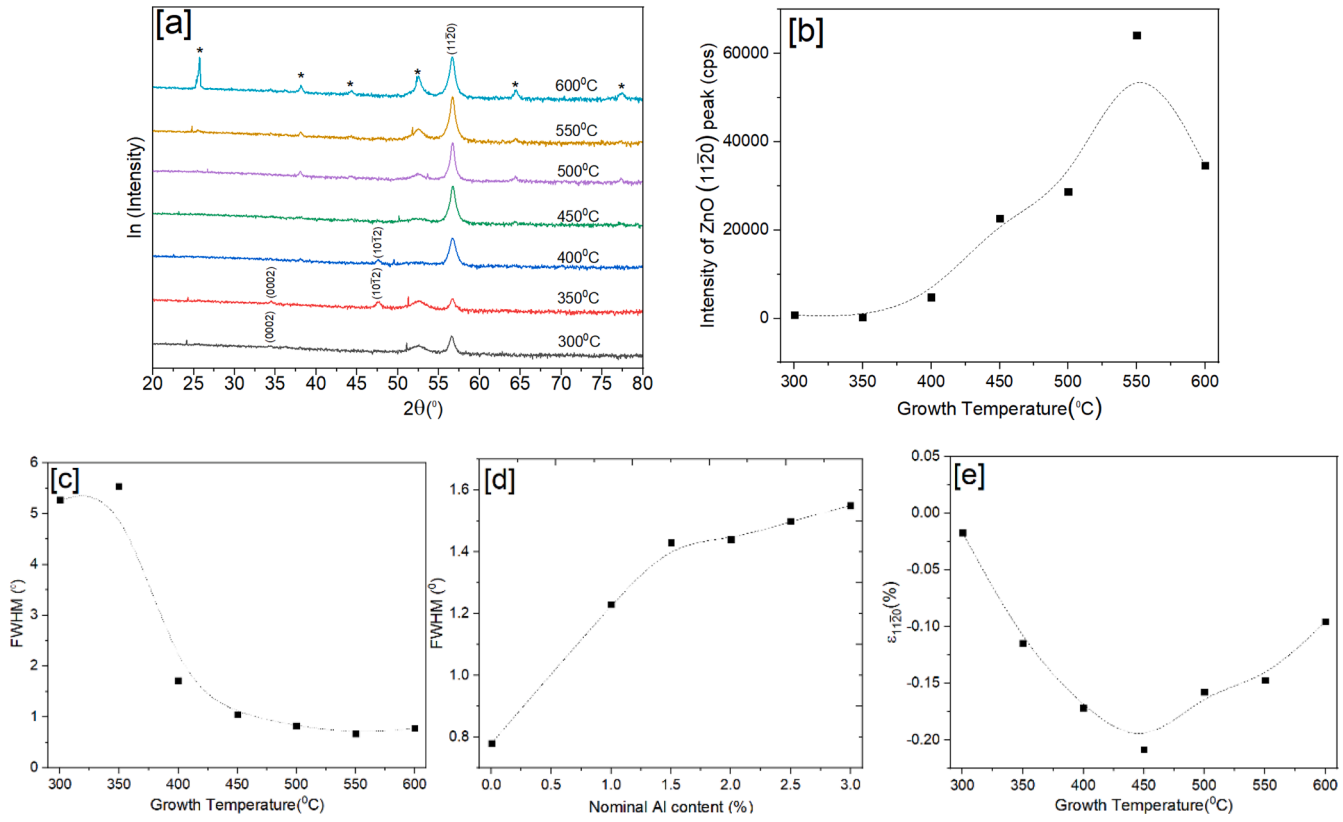


**Fig. 5.** (a) 2θ-ω scans of samples grown at different temperatures (* indicate substrate peaks); (b) intensity of the ZnO(11$\bar{2}$0) peak as a function of the growth temperature;(c) FWHM of the optimized ZnO(11$\bar{2}$0) peak as a function of the growth temperature; (d) FWHM of the (11$\bar{2}$0) peak of Al: ZnO as a function of the nominal aluminium concentration for samples grown at 450 °C; (e) compressive strain along the out-plane direction of a-ZnO as a function of the growth temperature. (The dotted lines do not represent a model fit; it is just intended as a visual aid to guide the eye.)

**Table 1**
Electrical characterisation results (resistivity, carrier concentration, mobility) of AZO samples grown at temperatures 450 °C and 500 °C with different nominal aluminium concentrations.

| Substrate temperature | 450 °C | | | 500 °C | | |
|---|---|---|---|---|---|---|
| Nominal Al mol% | Resistivity, ρ (Ω·cm) | Carrier concentration, n ($cm^{-3}$) | Mobility, μ ($cm^2/V·s$) | Resistivity, ρ (Ω·cm) | Carrier concentration, n ($cm^{-3}$) | Mobility, μ ($cm^2/V·s$) |
| 0 | 0.17745 | $6.069 \times 10^{18}$ | 5.796 | 0.92814 | $1.667 \times 10^{18}$ | 4.034 |
| 1 | 0.01196 | $5.0302 \times 10^{19}$ | 10.377 | 0.10583 | $5.118 \times 10^{18}$ | 11.52 |
| 1.5 | 0.0163 | $4.2298 \times 10^{19}$ | 9.053 | 0.04518 | $1.9077 \times 10^{19}$ | 7.2413 |
| 2 | 0.04052 | $2.26 \times 10^{19}$ | 6.8 | 0.03598 | $2.6554 \times 10^{19}$ | 6.5334 |
| 2.5 | 0.03831 | $3.596 \times 10^{19}$ | 4.531 | 0.05608 | $2.0361 \times 10^{19}$ | 5.4663 |
| 3 | 0.04028 | $3.0078 \times 10^{19}$ | 5.1524 | 0.10443 | $2.112 \times 10^{19}$ | 2.83 |

[23]. Aluminium has a low solubility of about 3–4 % in ZnO thin films. The resistivity depends on both the carrier concentration and the mobility. In general, the carrier concentration increases with the increase of aluminium nominal concentration in the precursor solution, then it decreases with a further increase in the aluminium nominal content. This decrease could be understood because of the segregation of $Al^{3+}$ dopants at the grain boundaries in the amorphous $Al_2O_3$. In undoped ZnO films, the charge carriers are due to intrinsic defects like zinc interstitials and oxygen vacancies. The significant increase in the charge carrier concentration with increasing doping is because the $Al^{3+}$ dopant is a more effective donor than intrinsic defects [24]. It can be seen that with a low concentration $Al^{3+}$ addition, the carrier mobility of the film is higher than that of undoped ZnO, however, further increase of aluminium content results in a decrease of the mobility. The decrease in mobility is because of the increase in the scattering, produced by the increased ionized impurities and the grain boundary.

The electrical measurement parameters of AZO grown at 450 °C and 500 °C temperatures were compared. The resistivity of samples grown at 450 °C was much lower than those grown at 500 °C (Fig. 6(c)). Since there is no significant difference in the mobility values (Fig. 6(e)), the decreased resistivity of the AZO samples grown at 450 °C is due to the higher charge carrier concentration of the samples compared to those grown at 500 °C (Fig. 6(d)). This may be explained by considering the thermal decomposition of the aluminium precursor. It has been reported that aluminium acetylacetonate decomposes between 160 °C and 220 °C, and the zinc acetate dihydrate completely decomposes at ~300 °C [25]. Now depending on the temperature profile above the substrate between the spray nozzle and the substrate, the precursors will decompose and will form the required material (ZnO and AZO in the respective cases) and adhere over the substrate. Now, when comparing growth at temperatures 450 °C and 500 °C, the aluminium precursor could decompose into its volatile form way earlier before reaching the substrate in the case of 500 °C, reducing the number of Aluminium atoms available for incorporation just above the substrate surface. Thus,

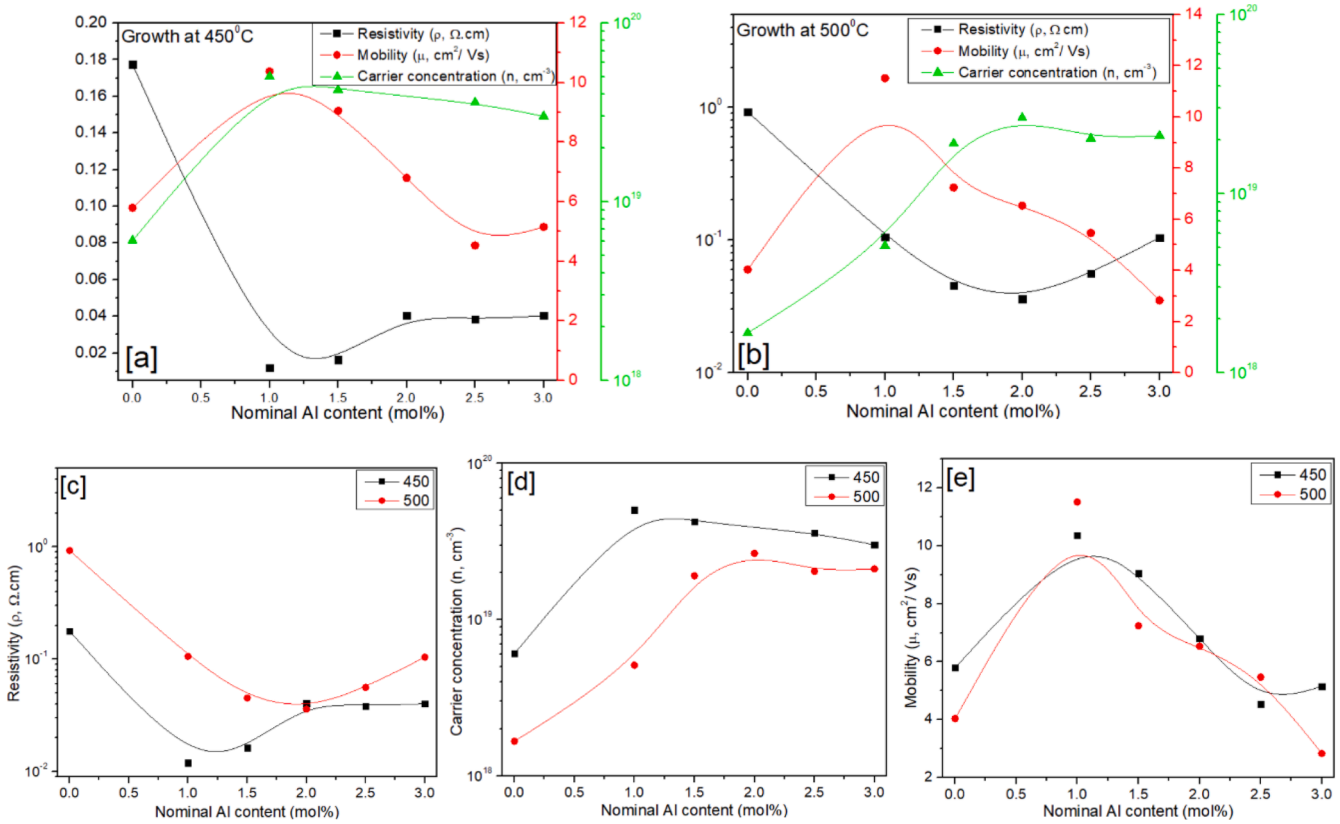


**Fig. 6.** Resistivity, charge carrier concentration and mobility as a function of the Aluminium concentration for samples grown at temperatures 450 °C (a) and 500 °C (b). Comparison between the variation of resistivity (c), charge carrier concentration (d) and mobility (e) for AZO samples grown at 450 °C and 500 °C.

more Aluminium will be available near to the substrate surface in the case of growth at 450 °C than that at 500 °C, because of which the carrier concentration will also be higher in the former case. This is represented in the schematic shown in Fig. 7. Another factor which could contribute is related to the desorption of Al compound from the surface. The Al precursor compound adsorbed at the surface, at higher temperatures will have higher thermal energy and thereby can get easily desorbed from the substrate surface. This increased desorption at higher temperatures also contributes to the reduced Al incorporation into the lattice.

In another study by T.Y. Ma and S.C. Lee [26], it was observed a similar behaviour, that is: the carrier concentration of nominal 1.4 wt%

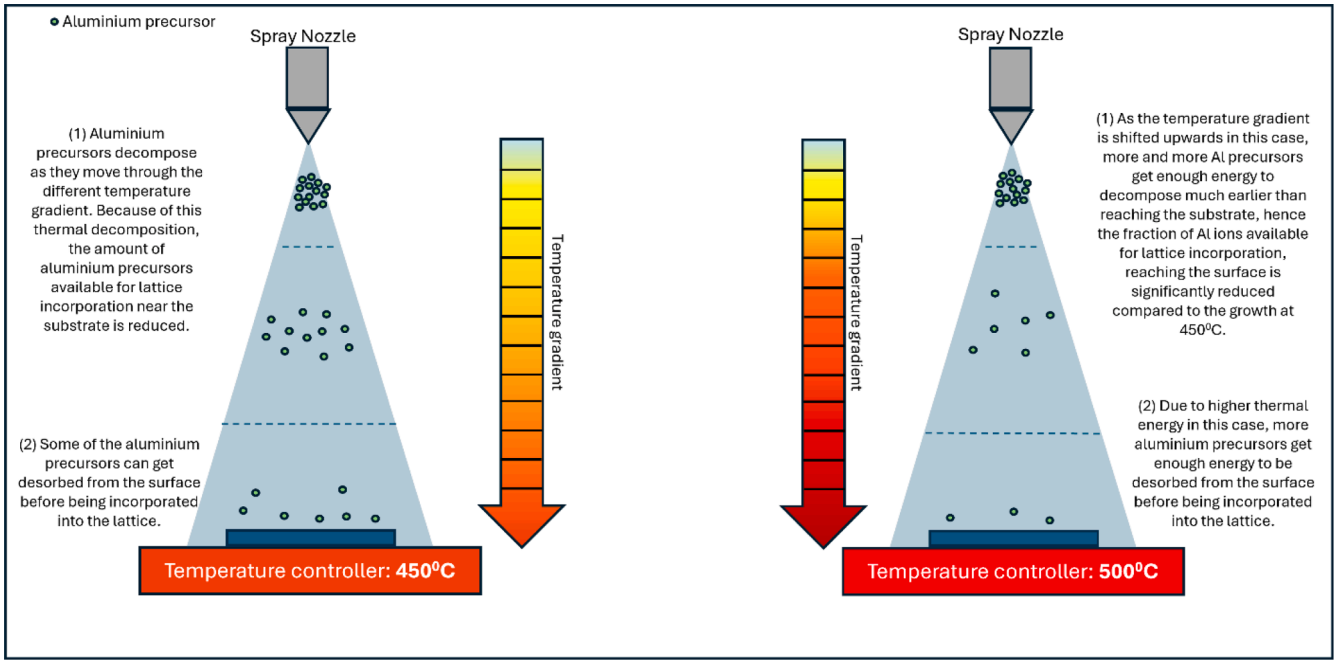


**Fig. 7.** Schematic of the mechanism proposed to explain the increased charge carrier concentration for samples grown at 450 °C, compared to that of 500 °C.

AZO increased with increasing substrate temperature until a certain point, after which it started to decline. They attributed this reduction in the carrier concentration to the reduction of Al atoms arriving to the substrate due to its reduction in the aerosol as a consequence of a higher reactor temperature [26]. The temperature at which this drop in this carrier concentration was observed is lower than the range used in our work. One possible reason for this difference is their use of ultrasonic spray pyrolysis; with the precursor solution delivered as a fine mist, the smaller droplet size likely led to faster decomposition of precursors than in our setup, where the spray nozzle generated the aerosol. Additionally, their use of aluminium chloride as the aluminium source, which completely decomposes at 200 °C [27], could contribute, as it is slightly lower than the decomposition temperature of aluminium acetyl acetonate (220 °C) used in our study.

The electrical properties of AZO films vary depending on the quality of the films which in turn depends on the deposition technique and the post-deposition treatments, which mainly affect the crystallinity and the microstructure of the thin films. Feng-Kuan Chen et al. reported the growth of (0002) oriented AZO with particle-like morphology with large hillocks with a charge carrier concentration of $10.33 \times 10^{20}$ $cm^{-3}$ with mobility of 9 $cm^2/V{\cdot}s$ using High vacuum dual target sputtering for AZO with Al/Zn=0.104 ratio, and after annealing in the presence of forming gas, they were able to reduce the resistivity from $3.19 \times 10^{-4}$ Ω·cm to $9.38 \times 10^{-5}$ Ω·cm by increasing the mobility to 20 $cm^2/V{\cdot}s$ [28]. S. Kuprenaite et al. synthesized epitaxial AZO with a smooth surface with ~2.7 at% aluminium with resistivity of $7.6 \times 10^{-4}$ Ω·cm, carrier concentration of $1.46 \times 10^{20}$ $cm^{-3}$ and high mobility of 56.5 $cm^2/$ V·s, but with a sophisticated aerosol-assisted MOCVD technique and on subsequent annealing the carrier concentration became $2.28 \times 10^{20}$ $cm^{-3}$ and mobility improved to 65.1 $cm^2/V{\cdot}s$ [24]. Similarly, M.J. Rivera et al. synthesized (0002) oriented AZO with round and hexagonal shaped agglomerates like morphology, with 3 at% aluminium content with resistivity of $4.3 \times 10^{-4}$ Ω·cm, carrier concentration of $3.7 \times 10^{20}$ $cm^{-3}$ and mobility of 7.4 $cm^2/V{\cdot}s$ using ultrasonic spray pyrolysis [25]. Using spray pyrolysis, A. Kumar et al. obtained a carrier concentration of $1.8 \times 10^{18}$ $cm^{-3}$ and mobility of 13 $cm^2/V{\cdot}s$ for as-deposited 1 at% AZO which was oriented in (0002) direction with particle like morphology and on vacuum annealing achieved carrier concentration of $1.7 \times 10^{20}$ $cm^{-3}$ and mobility of 50 $cm^2/V{\cdot}s$ [29]. W. Zhang et al. reported the growth of as-deposited 3 at% AZO using pulsed laser ablation with carrier concentration of $7.8 \times 10^{18}$ $cm^{-3}$ and mobility of 3.6 $cm^2/V{\cdot}s$, and on annealing the carrier concentration improved significantly to $1.1 \times 10^{21}$ $cm^{-3}$ and 10.7 $cm^2/V{\cdot}s$ [30]. In our work, the as-deposited AZO film with a nominal aluminium concentration of 1 % had a carrier concentration of $5.03 \times 10^{19}$ $cm^{-3}$ and mobility of 10 $cm^2/V{\cdot}s$. Achieving these levels in as-deposited films grown by a simple technique like spray pyrolysis without any additional thermal treatment, while having an excellent film morphology and good structural quality reflects the significance of our results.

## 4. Conclusions

We have successfully demonstrated the epitaxial growth of non-polar a-plane ZnO and aluminium-doped a-ZnO (AZO) thin films on r-sapphire substrates using our optimized homemade intermittent spray pyrolysis setup. The epitaxial relationships of the samples found from pole figure measurements were as follows: $ZnO(11\bar{2}0) \| Al_2O_3(01\bar{1}2)$, $ZnO[0001] \| Al_2O_3[01\bar{1}\bar{1}]$ and $ZnO[\bar{1}100] \| Al_2O_3[2\bar{1}\bar{1}0]$. The films had good morphology and were compact and uniform when the growth temperature was in the temperature range of 450 °C-500 °C. At both lower and higher growth temperatures the surface of the films was roughened because of the instability in the growth conditions due to the Ehrlich-Schwoebel effect and stress-induced instability, respectively. By using this low-cost and relatively simple set-up, we were able to grow epitaxial films with a structural quality comparable to the epitaxial films grown by well-established conventional techniques, like ultrasonic SP, aerosol-assisted MOCVD or High vacuum dual target sputtering, with higher operational costs and, in some cases, the needed of post-grown annealing processes. The variation of strain along the a-axis of the ZnO with the variation of growth temperature was also studied. The effect of aluminium doping on ZnO was investigated for growth temperatures 450 °C and 500 °C using morphological, structural and electrical (Hall measurements) characterisation. The electrical properties of the AZO samples grown at 450 °C (the lower temperature in the optimum temperature range for epitaxial growth) were better than those grown at 500 °C (the higher temperature in the optimum temperature range for epitaxial growth). This is explained by the difference in the availability of the Aluminium atoms present just above the surface of the substrate due to the difference in the temperature gradient profile above the substrate in both cases. As the temperature gradient profile (the temperature at which the aluminium precursor decomposes to its volatile form) would be shifted away from the substrate in the case of 500 °C than 450 °C, more Al precursor gets enough energy to decompose to its volatile form, much earlier than reaching the substrate. Therefore, the fraction of Al atoms reaching the substrate surface (available to be included in the lattice) is reduced in the case of 500 °C (the higher growth temperature) than that of 450 °C. Another contributing factor is the higher desorption rate of aluminium precursor at higher temperatures, which can contribute to the reduction in the number of Al ions available for lattice incorporation. Due to this, the amount of Al incorporated into the lattice is also lower in the case of 500 °C than that of 450 °C. The AZO sample with a nominal aluminium concentration of 1 % without any post-deposition treatments had a carrier concentration of $5.03 \times 10^{19}$ $cm^{-3}$ and mobility of 10 $cm^2/V{\cdot}s$. The successful epitaxial growth of non-polar a-plane ZnO and AZO with this low cost and simple technique of spray pyrolysis and that too with very good morphology, and good structural and electrical properties open a way to reduce the cost of production of this material in the frame of optoelectronic devices.

## CRediT authorship contribution statement

**Cerine Treesa Russel:** Writing – original draft, Visualization, Methodology, Investigation, Formal analysis, Data curation, Conceptualization. **Carmen Martinez Tomas:** Writing – review & editing, Visualization, Investigation, Formal analysis. **Vicente Muñoz Sanjosé:** Writing – review & editing, Supervision, Resources, Project administration, Methodology, Investigation, Funding acquisition, Conceptualization.

## Declaration of competing interest

The authors declare that they have no known competing financial interests or personal relationships that could have appeared to influence the work reported in this paper.

## Acknowledgements

This work was partially funded by the Spanish Ministry of Science and Innovation/AEI under Project PID2020-114796RB-C22/AEI/10.13039/501100011033; PDC2023-145827-C22/ AEI/10.13039/501100011033/European Union- NextGenerationEU/PRTR and the Generalitat Valenciana under Project PROMETEU/2021/066. Cerine Treesa Russel would like to thank the Generalitat Valencia for the financial support of her contract as PhD student. We would also like to thank Servei Central de Suport a la Investigacio Experimental (SCSIE), University of Valencia, for their instrumental facilities.

## Data availability

Data will be made available on request.

## References


[1] R. Triboulet, J. Perrière, Epitaxial growth of ZnO films, Prog. Crys. Growth Characteriz. Mater. 47 (2003) 65–138, https://doi.org/10.1016/j.pcrysgrow.2005.01.003.

[2] P. Pant, J.D. Budai, J. Narayan, Nonpolar ZnO film growth and mechanism for anisotropic in-plane strain relaxation, Acta Mater. 58 (2010) 1097–1103, https://doi.org/10.1016/j.actamat.2009.10.026.

[3] J. Chen, J. Zhang, J. Dai, F. Wu, S. Wang, H. Long, R. Liang, J. Xu, C. Chen, Z. Tang, Y. He, M. Li, Z. Feng, Strain dependent anisotropy in photoluminescence of heteroepitaxial nonpolar a-plane ZnO layers, Opt. Mater. Express. 7 (2017) 3944, https://doi.org/10.1364/ome.7.003944.

[4] C.W. Chen, S.C. Hung, C.H. Lee, C.J. Tun, C.H. Kuo, M.D. Yang, C.W. Yeh, C.H. Wu, G.C. Chi, Nonpolar light emitting diode made by m-plane n-ZnO/p-GaN heterostructure, Opt. Mater. Express. 1 (2011) 1555–1560, https://doi.org/10.1364/OME.1.001555.

[5] G. Tabares, A. Hierro, B. Vinter, J.-M. Chauveau, Polarization-sensitive Schottky photodiodes based on a-plane ZnO/ZnMgO multiple quantum-wells, Appl. Phys. Lett. 99 (2011) 071108, https://doi.org/10.1063/1.3624924.

[6] S. Mridha, D. Basak, Aluminium doped ZnO films: Electrical, optical and photoresponse studies, J. Phys. D: Appl. Phys. 40 (2007) 6902–6907, https://doi.org/10.1088/0022-3727/40/22/008.

[7] C.-Y. Peng, J.-S. Tian, W.-L. Wang, Y.-T. Ho, S.-C. Chuang, Y.-H. Chu, L. Chang, Effect of growth temperature on a-plane ZnO formation on r-plane sapphire, J. Vac. Sci. Technol. A. 29 (2011), https://doi.org/10.1116/1.3549141.

[8] K.W. Kim, H.S. Son, N.J. Choi, J. Kim, S.N. Lee, Growth and characterization of polar and nonpolar ZnO film grown on sapphire substrates by using atomic layer deposition, Thin Solid Films 546 (2013) 114–117, https://doi.org/10.1016/j.tsf.2013.03.071.

[9] S. Tanaka, Y. Ishikawa, T. Suzuki, N. Shibata, Photoluminescence from ZnO thin film deposited on R-Plane sapphire substrate by RF magnetron sputtering, Key Eng. Mater. 388 (2009) 19–22, https://doi.org/10.4028/www.scientific.net/kem.388.19.

[10] R. O'Haire, A. Meaney, E. McGlynn, M.O. Henry, J.R. Duclère, J.P. Mosnier, Growth of crystalline ZnO nanostructures using pulsed laser deposition, Superlattices Microstruct. 39 (2006) 153–161, https://doi.org/10.1016/j.spmi.2005.08.071.

[11] C.C. Zheng, S.J. Xu, J.Q. Ning, W. Bao, J.F. Wang, J. Gao, J.M. Liu, J.H. Zhu, X. L. Liu, Residual strains and optical properties of ZnO thin epilayers grown on r-sapphire planes, Semicond. Sci. Technol. 27 (2012) 035008, https://doi.org/10.1088/0268-1242/27/3/035008.

[12] S. Liang, C.R. Gorla, N. Emanetoglu, Y. Liu, W.E. Mayo, Y. Lu, Epitaxial growth of (1120) ZnO on (0112) Al2O3 by metalorganic chemical vapor deposition, J. Electron. Mater. 27-11 (1998) L72–L76, https://doi.org/10.1007/s11664-998-0083-6.

[13] G. Saraf, Y. Lu, T. Siegrist, In-plane anisotropic strain in a-ZnO films grown on r -sapphire substrates, Appl. Phys. Lett. 93 (2008) 041903, https://doi.org/10.1063/1.2965801.

[14] J.J. Chu, R.S. Liu, J.H. Kung, P.T. Wu, L.J. Chen, Epitaxial growth of high Tc superconducting Y-Ba-Cu-O thin films on (001)MgO by a chemical spray pyrolysis method, J. Appl. Phys. 64 (1988) 2523–2526, https://doi.org/10.1063/1.342497.

[15] A.A. Wernberg, D.J. Lawrence, H.J. Gysling, A.J. Fib, T.N. Blanton, Epitaxial growth of gallium arsenide thin films by spray pyrolysis using a single-source organometallic precursor, J. Cryst, Growth 131 (1993) 176–180, https://doi.org/10.1016/0022-0248(93)90411-O.

[16] S.-T. Zhang, J.-L. Rouvière, V. Consonni, H. Roussel, L. Rapenne, E. Pernot, D. Muñoz-Rojas, A. Klein, D. Bellet, High quality epitaxial fluorine-doped SnO2 films by ultrasonic spray pyrolysis: structural and physical property investigation, Mater. Des. 132 (2017) 518–525, https://doi.org/10.1016/j.matdes.2017.07.037.

[17] A. Ainabayev, B. Walls, D. Casey, D. Caffrey, D. Mullarkey, A. McGlinchey, A. Khare, A. Tikhonov, C. Ilhan, D. Brennan, S.J. McCormack, I. Shvets, Tailoring Epitaxial VO2 thin films with tunable properties via spray pyrolysis, J. Phys. Chem. C 127 (2023) 24432–24442, https://doi.org/10.1021/acs.jpcc.3c06057.

[18] Z.J. Liu, Y.G. Shen, Temperature effect on surface roughening of thin films, Surf. Sci. 595 (2005) 20–29, https://doi.org/10.1016/j.susc.2005.07.032.

[19] R. Rangdee, P. Chatraphorn, Effects of the Ehrlich-Schwoebel potential barrier on the Wolf-Villain model simulations for thin film growth, Surf. Sci. 600 (2006) 914–920, https://doi.org/10.1016/j.susc.2005.12.021.

[20] M.C. Martinez-Tomas, O. Klymov, K. Shimazoe, J.F. Sánchez-Royo, M. E. Changarath, S. Agouram, V. Muñoz-Sanjosé, Elastic and inelastic strain in submicron-thick ZnO epilayers grown on r-sapphire substrates by metal–organic vapour phase deposition, Acta Crystallogr. B Struct. Sci. Cryst. Eng. Mater. 80 (2024) 72–83, https://doi.org/10.1107/S2052520624000441.

[21] B.P. Zhang, K. Wakatsuki, N.T. Binh, N. Usami, Y. Segawa, Effects of growth temperature on the characteristics of ZnO epitaxial films deposited by metalorganic chemical vapor deposition, Thin Solid Films. 449 (2004) 12–19, https://doi.org/10.1016/S0040-6090Ž03.01466-4.

[22] H.F. Mcmurdie, M.C. Morris, E.H. Evans, B. Paretzkin, W. Wong-Ng, L. Ettlinger, Standard X-Ray diffraction powder patterns from the JCPDS research associateship, Powder Diffr. 1-2 (1986) 64–77, https://doi.org/10.1017/S0885715600011593.

[23] M. Gabás, A. Landa-Cánovas, J.Luis Costa-Krämer, F. Agulló-Rueda, A.R. González-Elipe, P. Díaz-Carrasco, J. Hernández-Moro, I. Lorite, P. Herrero, P. Castillero, A. Barranco, J.Ramón Ramos-Barrado, Differences in n-type doping efficiency between Al- and Ga-ZnO films, J. Appl. Phys. 113 (2013) 163709, https://doi.org/10.1063/1.4803063.

[24] S. Kuprenaite, T. Murauskas, A. Abrutis, V. Kubilius, Z. Saltyte, V. Plausinaitiene, Properties of In-, Ga-, and Al-doped ZnO films grown by aerosol-assisted MOCVD: Influence of deposition temperature, doping level and annealing, Surf. Coat. Technol. 271 (2015) 156–164, https://doi.org/10.1016/j.surfcoat.2014.12.052.

[25] M.J. Rivera, E.B. Ramírez, B. Juárez, J. González, J.M. García-León, L. Escobar-Alarcón, J.C. Alonso, Low temperature-pyrosol-deposition of aluminum-doped zinc oxide thin films for transparent conducting contacts, Thin Solid Films 605 (2016) 108–115, https://doi.org/10.1016/j.tsf.2015.11.053.

[26] T.Y. Ma, S.C. Lee, Effects of aluminum content and substrate temperature on the structural and electrical properties of aluminum-doped ZnO films prepared by ultrasonic spray pyrolysis, J. Mater. Sci: Mater. Electron. 11 (2000) 305–309, https://doi.org/10.1023/A:1008925315123.

[27] M. Hartman, O. Trnka, O. Šolcová, Thermal decomposition of aluminum chloride hexahydrate, Ind. Eng. Chem. Res. 44 (2005) 6591–6598, https://doi.org/10.1021/ie058005y.

[28] F.K. Chen, D.C. Tsai, Z.C. Chang, E.C. Chen, F.S. Shieu, Influence of Al content and annealing atmosphere on optoelectronic characteristics of Al:ZnO thin films, Appl. Phys. Mater. Sci. Process. 126 (2020) 743, https://doi.org/10.1007/s00339-020-03835-5.

[29] A. Kumar, M.I. Ahmad, Role of defects in the electronic properties of Al doped ZnO films deposited by spray pyrolysis, J. Mater. Sci. 57 (2022) 7877–7895, https://doi.org/10.1007/s10853-022-07136-5.

[30] W. Zhang, J. Gan, L. Li, Z. Hu, L. Shi, N. Xu, J. Sun, J. Wu, Tailoring of optical and electrical properties of transparent and conductive Al-doped ZnO films by adjustment of Al concentration, Mater. Sci. Semicond. Process. 74 (2018) 147–153, https://doi.org/10.1016/j.mssp.2017.10.028.